

SIGNALS OF HEAVY MAJORANA NEUTRINOS AT HADRON COLLIDERS

O. PANELLA^{*§}, M. CANNONI^{¶§}, C. CARIMALO[‡] and Y. N. SRIVASTAVA^{¶§}.

[§]*Istituto Nazionale di Fisica Nucleare, Sezione di Perugia, Via A. Pascoli, I-06123 Perugia, Italy*

[¶]*Dipartimento di Fisica, Università degli Studi di Perugia, Via A. Pascoli, I-06123, Perugia, Italy*

[‡]*Laboratoire de Physique Nucléaire et Hautes Energies, IN2P3-CNRS*

Université Pierre et Marie Curie, 4 place Jussieu, Tour 33, F-75252, Paris Cedex 05, France

(November 2, 2018)

Abstract

The lepton number violating signal of like-sign-dileptons (LSD), $pp \rightarrow \ell^\pm \ell^\pm + 2\text{jets}$, is investigated within a model of mixing in the neutrino sector assuming the existence of heavy Majorana neutrino states with a left-handed coupling to the light leptons. The LSD signal receives contributions both from the resonant production of a heavy Majorana neutrino (N) and from the exchange of a virtual N in the WW fusion mechanisms. These two possibilities are discussed in detail and compared. Helicity amplitudes are given pointing out differences with calculations previously reported by other authors. The signal cross-sections are computed at the energy of the LHC collider ($\sqrt{S} = 14$ TeV) at CERN and within the existing experimental limits on the mixing couplings, including those coming from neutrinoless double beta decay. Detailed angular distributions of signal reactions which are complementary to previous studies on the argument are presented.

12.60.-i, 13.15.+g, 14.60.St, 23.40.-s

Typeset using REVTeX

*Author to whom correspondence should be addressed. E-mail: Orlando.Panella@PG.infn.it

I. INTRODUCTION

The quest for a complete understanding of the true nature of neutrino masses and mixing in the neutrino sector of the Standard Model (SM) is one of the most important challenges that physicists have to face in the coming years. Perhaps the experimental difficulties involved in the study of neutrino properties can be best appreciated noticing that only very recently the neutral partner of the tau lepton, the tau neutrino (ν_τ), has been directly observed [1]. In addition, after decades of experimental efforts there is finally some evidence for neutrino oscillations [2] and thus the first indications of the fact that neutrinos might not be massless particles as advocated by the SM. Even so, it is not clear at present whether these neutral fermions are of Dirac or Majorana type (for a Dirac neutral $\nu \neq \bar{\nu}$ while for a Majorana $\nu = \bar{\nu}$). It is well known that if neutrinos are of the Majorana type then the Lepton number (L) is not conserved and processes which violate L by two units $\Delta L = \pm 2$ become possible. Perhaps one of the most interesting lepton number violating processes is the neutrinoless double beta decay $\beta\beta_{0\nu}$ which currently provides the most stringent bound on the *effective light* Majorana mass $\langle m_\nu \rangle \leq 0.1$ eV. Extensive literature is available on this subject both from the experimental and theoretical sides. In view of the forthcoming large hadron collider (LHC) to be built at CERN which will realize proton–proton collisions at energies of $\sqrt{S} = 14$ TeV it will be of increasing importance to study quark reactions which are the high–energy analogues of the $\beta\beta_{0\nu}$. This was realized already some time ago and has been the object of several studies of the signal (lepton number violating) reaction:

$$pp \rightarrow \ell^\pm \ell^\pm + 2 \text{ jets} \quad (\Delta L = \pm 2). \quad (1)$$

Any model with lepton number violation (i.e. due to the presence of massive Majorana neutrinos) will provide a non zero amplitude for the process in Eq. 1, which receives contributions from parton scattering as depicted in Fig. 1 and Fig. 2. In a series of recent papers [3–6], the present authors have addressed the question of lepton number violation within a composite model scenario where the partner of the light neutrino, the so called

excited neutrino, N , is assumed to be of a Majorana type. The phenomenological implications of this idea have been investigated in detail both with respect to the low-energy $\beta\beta_{0\nu}$ decay and to the high-energy LSD signal in hadron collisions. In particular, in [6] we developed a helicity amplitude method to efficiently compute all $2 \rightarrow 4$ parton subprocesses that contribute to the reaction in Eq. (1). The cross-sections were estimated to lead, within some regions of the parameter space, to an observable signal. One particular advantage of the approach developed in [6] is that it gives the possibility to treat coherently the two mechanisms of WW-fusion and resonant production (annihilation channel). Clearly such an approach can be extended to explore the phenomenology of other models that entail L violation. In the event of observation of such a signal, it will be important to know the contribution to it of the various models beyond the SM and ultimately, a way to distinguish among them to understand the responsible mechanism .

In this work, the model of heavy isosinglets Majorana states that mix with ordinary light lepton via a left-handed coupling suppressed by a mixing coefficient, is assumed and studied in detail. While completing this work a report [7] appeared in the literature which also commented upon the same model of heavy Majorana neutrinos by studying the resonant production at LHC via the third order process

$$pp \rightarrow \ell^+ \ell^+ + W^- \quad \Delta L = +2 \quad (2)$$

and arriving at somewhat optimistic results as to the possibility of observing the signal. The process in Eq. (2) is described by the Feynman diagram obtained by that of Fig. 2 but without including the hadronic decay products of the final *on-shell* W . However, the method used here of evaluating analytically all the relevant amplitudes, as developed in [6], is totally independent of that of the authors of [7] which relies on the COMPHEP [8] package. The rest of the paper is organized as follows: section II gives a description of the theoretical framework; in section III the amplitudes of the contributing subprocesses are presented; in section IV an exact analytic result is provided for the process in Eq. 2 highlighting differences with the formula reported in [7] and discussing thoroughly how the conclusions

reported there are affected; section V presents some discussion of kinematic cuts and gives some details of the numerical calculations along with the results; finally section VI provides concluding remarks.

II. THE MODEL

The mixing of heavy and light neutrinos is a common feature of many theoretical models beyond the SM. Heavy Majorana neutral leptons have been well studied in the literature in particular from a model which is the SM augmented with additional right-handed neutrino fields. In this scenario, that can be seen as a low-energy manifestation of $SU(10)$ GUT theories [9,10], one has the following mass term for neutrinos:

$$\mathcal{L}_{mass} = -\frac{1}{2} \left(\bar{\nu}_L \overline{(\nu_R)^c} \right) \mathcal{M} \begin{pmatrix} (\nu_L)^c \\ \nu_R \end{pmatrix} + h.c. , \quad (3)$$

where $(\nu_L)^c$ and ν_R are vectors in generation space with components given by three chiral fields:

$$(\nu_L)^c = \begin{pmatrix} (\Psi_L^{\nu_e})^c \\ (\Psi_L^{\nu_\mu})^c \\ (\Psi_L^{\nu_\tau})^c \end{pmatrix} \quad \nu_R = \begin{pmatrix} \Psi_R^{\nu_e} \\ \Psi_R^{\nu_\mu} \\ \Psi_R^{\nu_\tau} \end{pmatrix} , \quad (4)$$

and a mass matrix given by

$$\mathcal{M} = \begin{pmatrix} 0 & M_D \\ M_D^T & M_R \end{pmatrix} . \quad (5)$$

In general an arbitrary number of right-handed neutrinos can be added, but for definiteness and simplicity the most symmetrical case is considered (i.e. that of three right-handed fields). The mass matrix is then 6×6 , with M_D the 3×3 matrix of Dirac type masses for neutrinos that is built via the spontaneous symmetry breaking and Yukawa couplings as for charged leptons and quarks, while M_R is the Majorana 3×3 mass matrix for singlet right-handed fields. If one requires the eigenvalues of M_R to be much bigger than those of M_D ,

diagonalizing the mass term one has a three generation “see-saw” [11,12] model, with three light and three heavy Majorana mass eigenstates. Weak interactions produce weak eigenstates that are superpositions of mass eigenstates through the mixing matrix. As opposed to the naive one family “see-saw” mechanism, where $\theta \simeq \sqrt{m_\nu/M_N}$, with three generations (or more) of right-handed neutrino fields, it is possible to decouple the magnitude of the mixing coefficient of heavy-light states from the mass eigenvalues of M_R , and the mixing angles can be treated as phenomenological parameters bounded only by existing experimental data. Examples of mass matrices that satisfy this request are given in ref. [13,14,9,15]. In this context, lepton number violation in pp collisions was analyzed in [16,13,17]. Some authors refer instead to other theoretical scenarios [7,18] derived from super-string inspired E_6 models. Here global symmetries imposed on the mass matrix decouple the mixing angles from any relation with masses eigenvalues, so that they are free parameters that can be large (as in multi-generational “see-saw” type models). Some caution however must be paid in deriving heavy Majorana masses in these models where every family of the SM is enlarged both with a right-handed field and a singlet field S_L in the neutrino sector. The mass term for neutrinos in the Lagrangian is [19–21]:

$$\mathcal{L}_{mass} = -\frac{1}{2} \left(\bar{\nu}_L \quad \overline{(\nu_R)^c} \quad \bar{S}_L \right) \mathcal{M} \begin{pmatrix} (\nu_L)^c \\ \nu_R \\ S_L^c \end{pmatrix} + h.c. , \quad (6)$$

where the mass matrix is given by:

$$\mathcal{M} = \begin{pmatrix} 0 & D & 0 \\ D^T & 0 & M^T \\ 0 & M & 0 \end{pmatrix} , \quad (7)$$

where again the fields represent a collection of three chiral fields and the block M and D are Dirac type sub-matrices. The zeros are consequence of the global lepton number conservation imposed on the mass matrix. The spectrum that one obtains through diagonalization is three massless neutrinos and three heavy Dirac neutral leptons [22]. Therefore these type

of models cannot be the base for the discussion of the lepton violating processes that are the object of this work. One could add a Majorana mass matrix, μ for S_L [23] (lower left 3×3 block in the mass matrix of Eq. (7)), and obtain a small Majorana mass for the light neutrinos, but the heavy states remain Dirac particles. Thus in this class of models it is not very easy to obtain heavy Majorana masses (in the TeV range) with substantial heavy-light mixing.

Independent of theoretical prejudices, in the following the general interaction Lagrangian between charged leptons, neutrinos, and gauge vector bosons of the SM is given within this class of models where the weak eigenstate neutrinos are combinations through the mixing matrix of light and heavy *physical* neutrinos. So the latter have the usual left-handed coupling with leptons with a coupling constant that is the SM weak coupling g multiplied by the appropriate element of the mixing matrix. The charged and neutral current interaction Lagrangian densities are given by:

$$\begin{aligned} \mathcal{L}_{int}^{cc} &= -\frac{g}{\sqrt{2}} \sum_{\ell=e,\mu,\tau} \left\{ \sum_i \bar{\Psi}_\ell \gamma^\mu \frac{1-\gamma^5}{2} (B_{\ell\nu})_{\ell i} \Psi_{\nu i} \right. \\ &\quad \left. + \sum_j \bar{\Psi}_\ell \gamma^\mu \frac{1-\gamma^5}{2} (B_{\ell N})_{\ell j} \Psi_{N j} \right\} W_\mu^- + h.c. \\ \mathcal{L}_{int}^{nc} &= -\frac{g'}{2 \sin \theta_W} Z^\mu \sum_{i,j} \bar{\Psi}_{\nu i} \gamma_\mu \frac{1-\gamma^5}{2} C_{ij} \Psi_{\nu j} \end{aligned} \quad (8)$$

where $B_{\ell n}$ is a 3×6 rectangular mixing matrix that can be written $B_{\ell n} = (B_{\ell\nu}, B_{\ell N})$, with $B_{\ell\nu}$ and $B_{\ell N}$ the two 3×3 block matrices that give the light-light and light-heavy mixing, while the 6×6 matrix C_{ij} is given by $C = B^\dagger B$. The properties of B and C are extensively discussed in the literature [24–26]. We now discuss the known experimental constraints on mixing angles. As these heavy states have not yet been observed, light-heavy mixing has to be inferred by low-energy phenomenology. In [27], a global fit is performed on LEP data identifying the following effective mixing angles:

$$\begin{aligned} c_{\nu_\ell}^2 &= (B_{\ell\nu}^\dagger B_{\ell\nu})_{\ell\ell} = \sum_i |(B_{\ell\nu})_{i\ell}|^2 \equiv \cos^2 \theta_{\nu_\ell}, \\ s_{\nu_\ell}^2 &= (B_{\ell N} B_{\ell N}^\dagger)_{jj} = \sum_j |(B_{\ell N})_j|^2 \equiv \sin^2 \theta_{\nu_\ell} \end{aligned}$$

$$= 1 - c_{\nu_\ell}^2 = 1 - \sum_{i=1}^3 |B_{\ell\nu_i}|^2 = \sum_{j=4}^6 |B_{\ell N_j}|^2, \quad (9)$$

that are bounded from above as:

$$s_{\nu_e}^2 < 0.005 \quad s_{\nu_\mu}^2 < 0.002 \quad s_{\nu_\tau}^2 < 0.01. \quad (10)$$

The authors of ref. [7] have performed an updated analysis finding roughly the same value for the bound on the electron parameter $s_{\nu_e}^2 < 0.0052$ but a somewhat more stringent bound on the muon mixing parameter $s_{\nu_\mu}^2 < 0.0001$, thereby making the electron LSD channel the most interesting. However for first generation leptons it is necessary to consider bounds coming from non observation of neutrinoless double beta decay (see below). In the next sections calculations are reported for the first family ($\ell = e$) LSD signal under the assumption that: *i*) only one heavy Majorana eigenstate is exchanged; *ii*) the maximum allowed value for the mixing can be used for the relative element of the mixing matrix, i.e. $|B_{eN}|^2 = 0.0052$. It should be recalled that when extensions of the SM are embedded in more general theories, one needs to consider new gauge bosons that can interact with the heavy neutrino states. However, as these bosons are predicted to be very heavy, their interactions are suppressed relative to those of the SM so that one can safely neglect them [7,9] in the following discussion.

A. Unitarity and $\beta\beta_{0\nu}$ constraints

Before entering into the detailed calculations, a comment is in order, regarding violation of unitarity, and the bound coming from the non observation of neutrinoless double beta decay ($\beta\beta_{0\nu}$) which is quite important. It is well known [16,28,18] that the basic process $e^-e^- \rightarrow W^-W^-$ or, equivalently, $W^-W^- \rightarrow e^-e^-$ intervening in the reactions discussed in the present work (see Fig. 1), violates unitarity unless the following condition is satisfied:

$$\sum_{\nu} m_{\nu} (B_{\ell\nu})^2 + \sum_N M_N (B_{\ell N})^2 = 0. \quad (11)$$

In the model considered here this is automatically satisfied as it is easily shown that $\sum_{\nu} m_{\nu} (B_{\ell\nu})^2 + \sum_N M_N (B_{\ell N})^2 = M_{\ell\ell}$ where $M_{\ell\ell}$ is the left-Majorana mass matrix (3×3 block matrix) of ν_{ℓ} , and this is zero as can be inferred from the mass matrix given in Eq. (5). The Majorana mass term of ν_{ℓ} could be different from zero within a Higgs triplet model which however has been excluded by the precision LEP data, unless one considers somewhat more contrived models, where, for example, the Higgs triplet is mixed with a singlet allowing to evade the LEP bounds [29]. In the following such eventualities are not considered, the absence of a Higgs triplet is assumed, ensuring thus the unitarity condition to be satisfied according to Eq. (5).

The non observation of the neutrinoless double beta decay (a second order weak nuclear decay) gives the following bound on the *effective inverse mass* [28]:

$$\left| \sum_N \frac{B_{eN}^2}{M_N} \right| < 7 \times 10^{-5} \text{ TeV}^{-1}, \quad (12)$$

Within the rather reasonable hypothesis that only the light mass eigenstate contributes significantly to both the low-energy ($\beta\beta_{0\nu}$) process and high-energy (LSD) signal and using $|B_{eN}|^2 \simeq 0.0052$ one easily finds a rather impressive lower bound on the mass [28]:

$$M_N > 75 \text{ TeV}. \quad (13)$$

This of course would preclude the possibility of producing such particles at any forthcoming hadron or lepton collider. The $\beta\beta_{0\nu}$ bound could obviously be evaded as the mixing coefficients appear as squared and not through their moduli squared in Eq (12). Indeed in ref. [28] several scenarios of mixing are discussed where cancellations between different terms arise thus evading the $\beta\beta_{0\nu}$ bound. Explicit examples are provided [28] but of course the resulting models appear somewhat fine tuned and/or too much contrived and un-natural. It would then appear that a phenomenological analysis of the processes discussed in the introduction would be pointless for heavy neutrino masses within the mass range $100 \text{ GeV} \leq M_N \leq 1 \text{ TeV}$. However, one can build models which do not suffer such drawbacks of fine tuning and unnaturalness by simply assuming that the heavy Majorana

neutrinos do not have the same CP parities (η_{CP}). This was done by the authors of ref. [18] who considered a model with two degenerate heavy Majorana neutrinos of $M_N \approx 1$ TeV and opposite CP parities that evades the $\beta\beta_{0\nu}$ bound [18]. It is within such a scenario that the following phenomenological study of the processes in Eq. (2) and Eq. (1) has to be understood.

In any case it must be kept in mind that the predictions reported here are based on the maximum experimentally allowed mixing and therefore new global fits on the last LEP data may lower its value, and thus affect the present conclusions.

III. AMPLITUDES OF L-VIOLATING PARTON SUBPROCESS

In the following, the helicity amplitudes for parton sub-processes that contribute to production of LSD via the exchange (or production) of a heavy Majorana neutrino are presented. The effective interaction used is that of Eq. (8). Considering for the moment only the first family, three different types of processes should be distinguished: (i) $uu \rightarrow dd + \ell^+ \ell^+$, (ii) $u\bar{d} \rightarrow d\bar{u} + \ell^+ \ell^+$, (iii) $\bar{d}\bar{d} \rightarrow \bar{u}\bar{u} + \ell^+ \ell^+$.

Let the tensor $T_{\mu\nu}$ describe the virtual sub-process $W^*W^* \rightarrow \ell^+\ell^+$ (Fig. 1), while the tensor $\tilde{T}_{\mu\nu}$ describes the virtual sub-process $(W^*)^+ \rightarrow \ell^+\ell^+(W^*)^-$ appearing in the diagram of Fig. 2. $J_{a,c}$ and $\bar{J}_{b,d}$, are the quark (anti-quark) currents that couple in the t-channel to the virtual gauge bosons of the standard model (Fig. 1) while $\tilde{J}_{a,b}$ and $\tilde{J}_{c,d}^*$, are the incoming and outgoing currents of the $q\bar{q}'$ pair that couples in the s-channel to the W-bosons (Fig. 2):

$$\begin{aligned} J_{a,c}^\mu &= \bar{u}(p_c) \gamma^\mu P_L u(p_a) & \bar{J}_{b,d}^\mu &= \bar{v}(p_b) \gamma^\mu P_L v(p_d) \\ \tilde{J}_{a,b}^\mu &= \bar{v}(p_b) \gamma^\mu P_L u(p_a) & (\tilde{J}_{c,d}^\mu)^* &= \bar{u}(p_c) \gamma^\mu P_L v(p_d) \end{aligned} \tag{14}$$

with $P_L = (1 - \gamma_5)/2$.

With the following definitions of propagator factors:

$$\begin{aligned} 1/A &= [(p_a - p_c)^2 - M_W^2] [(p_b - p_d)^2 - M_W^2] \\ 1/B &= [(p_a - p_d)^2 - M_W^2] [(p_b - p_c)^2 - M_W^2] \end{aligned}$$

$$1/\tilde{A} = [(p_a + p_b)^2 - M_W^2 + iM_W\Gamma_W] [(p_c + p_d)^2 - M_W^2 + iM_W\Gamma_W] \quad (15)$$

$$\begin{aligned} C &= (p_a - p_c - p_e)^2 - M_N^2 & D &= (p_a - p_c - p_f)^2 - M_N^2 \\ E &= (p_a - p_d - p_e)^2 - M_N^2 & F &= (p_a - p_d - p_f)^2 - M_N^2 \\ \tilde{C} &= (p_a + p_b - p_e)^2 - M_N^2 + iM_N\Gamma_N & \tilde{D} &= (p_a + p_b - p_f)^2 - M_N^2 + iM_N\Gamma_N \end{aligned} \quad (16)$$

the amplitudes (in the unitary gauge) are :

$$(i) \quad \underline{U_i U_j \rightarrow D_k D_l + \ell^+ \ell^+}$$

$$\mathcal{M} = \mathcal{K} \left\{ V_{U_i D_k}^* V_{U_j D_l}^* A \left[J_{(a,c)}^\mu T_{\mu\nu} J_{(b,d)}^\nu \right] - V_{U_i D_l}^* V_{U_j D_k}^* B \left[(p_c \leftrightarrow p_d) \right] \right\}; \quad (17)$$

$$(ii) \quad \underline{U_i \bar{D}_j \rightarrow D_k \bar{U}_l + \ell^+ \ell^+}$$

$$\begin{aligned} \mathcal{M}(WW - \text{fusion}) &= \mathcal{K} (V_{U_i D_k})^* (V_{U_l D_j})^* \left[A J_{(a,c)}^\mu T_{\mu\nu} \bar{J}_{(b,d)}^\nu \right]; \\ \mathcal{M}(q\bar{q}' - \text{annihilation}) &= \mathcal{K} (V_{U_i D_j})^* (V_{U_l D_k})^* \left[\tilde{A} \tilde{J}_{(a,b)}^\mu \tilde{T}_{\mu\nu} (\tilde{J}_{(c,d)}^\nu)^* \right]; \end{aligned} \quad (18)$$

$$(iii) \quad \underline{\bar{D}_i \bar{D}_j \rightarrow \bar{U}_k \bar{U}_l + \ell^+ \ell^+}$$

$$\mathcal{M} = \mathcal{K} \left\{ V_{U_k D_i}^* V_{U_l D_j}^* A \left[\bar{J}_{(a,c)}^\mu T_{\mu\nu} \bar{J}_{(b,d)}^\nu \right] - V_{U_l D_i}^* V_{U_k D_j}^* B \left[(p_c \leftrightarrow p_d) \right] \right\}; \quad (19)$$

where U_i denotes a positively charged quark (up-type) while D_i denotes a negatively charged one (down-type). The quantities $V_{U_i D_j}$ are the elements of the CKM mixing matrix. Of course the annihilation diagram of Fig. 2 comes in only in quark-anti-quark scattering. In processes (i) and (iii) the part of the amplitude depending on the factor B is due to the diagrams obtained upon exchanging the final state quarks. In the framework of the Lagrangian c.f. Eq. (8), as discussed in section II, we have:

$$\begin{aligned} T_{\mu\nu} &= \bar{u}(p_e) \left[\frac{\gamma_\mu \gamma_\nu}{C} + \frac{\gamma_\nu \gamma_\mu}{D} \right] \frac{1 - \gamma_5}{2} v(p_f), \\ \tilde{T}_{\mu\nu} &= \bar{u}(p_e) \left[\frac{\gamma_\mu \gamma_\nu}{\tilde{C}} + \frac{\gamma_\nu \gamma_\mu}{\tilde{D}} \right] \frac{1 - \gamma_5}{2} v(p_f), \\ \mathcal{K} &= \frac{g^4}{4} (B_{eN})^2 M_N. \end{aligned} \quad (20)$$

Due to the chiral nature of the couplings involved, the calculation is particularly simple if performed in the helicity basis [30]. Within this approach the amplitudes are evaluated in

terms of *scalar spinor products* instead of scalar products of particle's momenta as in the usual method of squaring the amplitudes. In the massless approximation (all $p_i^2 = 0$ for external particles) the only non zero scalar products between spinors of given helicity are the quantities:

$$\begin{aligned} s(m, n) &= s(p_m, p_n) = \bar{u}_+(p_m)u_-(p_n), \\ t(m, n) &= t(p_m, p_n) = \bar{u}_-(p_m)u_+(p_n), \end{aligned} \quad (21)$$

which are given by:

$$\begin{aligned} s(m, n) &= -2\sqrt{E_m E_n} G_{mn}, \\ t(m, n) &= +2\sqrt{E_m E_n} F_{mn}, \end{aligned} \quad (22)$$

with:

$$\begin{aligned} G_{mn} &= \cos(\theta_m/2) \sin(\theta_n/2) e^{+i(\phi_m - \phi_n)/2} - \sin(\theta_m/2) \cos(\theta_n/2) e^{-i(\phi_m - \phi_n)/2}, \\ F_{mn} &= (G_{mn})^*. \end{aligned} \quad (23)$$

Consider for a moment the lepton line and its corresponding tensor $T_{\mu\nu}$ projected out on the helicity basis:

$$T_{\mu\nu}^{(\lambda, \lambda')}(p_e, p_f) = \bar{u}_\lambda(p_e) \left[\frac{\gamma_\mu \gamma_\nu}{C} + \frac{\gamma_\nu \gamma_\mu}{D} \right] \frac{1 - \gamma_5}{2} v_{\lambda'}(p_f) \quad (24)$$

It is easily shown (use $v_\lambda(p) = -2\lambda\gamma_5 u_{-\lambda}(p)$) that only one of the four helicity combinations is non vanishing:

$$\begin{aligned} T_{\mu\nu}^{(+,+)}(p_e, p_f) &= 0 & T_{\mu\nu}^{(-,-)}(p_e, p_f) &= 0 \\ T_{\mu\nu}^{(-,+)}(p_e, p_f) &= 0 & T_{\mu\nu}^{(+,-)}(p_e, p_f) &= \bar{u}_+(p_e) \left[\frac{\gamma_\mu \gamma_\nu}{C} + \frac{\gamma_\nu \gamma_\mu}{D} \right] u_-(p_f) \end{aligned} \quad (25)$$

In particular it follows that if $p_e = p_f = p$ then $C = D$ and:

$$T_{\mu\nu}^{(+,-)}(p, p) = 2 \frac{\eta_{\mu\nu}}{C} \bar{u}_+(p)u_-(p) = s(p, p) = 0. \quad (26)$$

Due to the structure of the coupling the two massless (identical) leptons have the same helicity and therefore by the Pauli exclusion principle if they have the same momentum

the amplitude must vanish. All amplitudes given below satisfy this property. The above remarks apply as well to the quark lines and in the massless approximation only one helicity amplitude is non zero. The following result is found:

(i) $U_i U_j \rightarrow D_k D_l + \ell^+ \ell^+$

$$\mathcal{M} = 4 \mathcal{K} t(c, d) \left\{ (V_{U_i D_k})^* (V_{U_j D_l})^* A \left[\frac{s(e, a) s(b, f)}{C} - \frac{s(f, a) s(b, e)}{D} \right] + (V_{U_i D_l})^* (V_{U_j D_k})^* B \left[\frac{s(e, a) s(b, f)}{E} - \frac{s(f, a) s(b, e)}{F} \right] \right\}, \quad (27)$$

(ii) $U_i \bar{D}_j \rightarrow D_k \bar{U}_l + \ell^+ \ell^+$

$$\mathcal{M} = 4 \mathcal{K} t(c, b) \left\{ (V_{U_i D_k})^* (V_{U_l D_j})^* A \left[\frac{s(e, a) s(d, f)}{C} - \frac{s(f, a) s(d, e)}{D} \right] + (V_{U_i D_j})^* (V_{U_l D_k})^* \tilde{A} \left[\frac{s(e, a) s(d, f)}{\tilde{C}} - \frac{s(f, a) s(d, e)}{\tilde{D}} \right] \right\}, \quad (28)$$

(iii) $\bar{D}_i \bar{D}_j \rightarrow \bar{U}_k \bar{U}_l + \ell^+ \ell^+$

$$\mathcal{M} = 4 \mathcal{K} t(a, b) \left\{ (V_{U_k D_i})^* (V_{U_l D_j})^* A \left[\frac{s(e, c) s(d, f)}{C} - \frac{s(f, c) s(d, e)}{D} \right] - (V_{U_l D_i})^* (V_{U_k D_j})^* B \left[\frac{s(e, d) s(c, f)}{E} - \frac{s(f, d) s(c, e)}{F} \right] \right\}. \quad (29)$$

The above simple analytic form of the amplitudes is also quite easy to implement in a code for numerical applications, since the quantities $s(p_i, p_j)$ and $t(p_i, p_j)$ are just functions of the energies and angles of the particle's momenta, c.f. Equations (22) and (23).

In addition it is also possible to derive from the above expression of the amplitudes the average squared matrix elements for the various processes in terms of scalar products of particle's four momenta. One finds using $|s(p_i, p_j)|^2 = |t(p_i, p_j)|^2 = 2p_i \cdot p_j$:

(i) $U_i U_j \rightarrow D_k D_l + \ell^+ \ell^+$

$$\sum |\mathcal{M}|^2 = 128 \mathcal{K}^2 |V_{U_i D_k}^* V_{U_j D_l}^*|^2 p_c \cdot p_d \left\{ p_a \cdot p_e p_b \cdot p_f \left| \frac{A}{C} + \xi_1^* \frac{B}{E} \right|^2 + p_a \cdot p_f p_b \cdot p_e \left| \frac{A}{D} + \xi_1^* \frac{B}{F} \right|^2 - L(p_a, p_f, p_b, p_e) \Re X_1 + \varepsilon(p_a, p_f, p_b, p_e) \Im X_1 \right\} \quad (30)$$

(ii) $U_i \bar{D}_j \rightarrow D_k \bar{U}_l + \ell^+ \ell^+$

$$\sum |\mathcal{M}|^2 = 128 \mathcal{K}^2 |V_{U_i D_k}^* V_{U_l D_j}^*|^2 p_c \cdot p_b \left\{ p_a \cdot p_e p_d \cdot p_f \left| \frac{A}{C} + \xi_2^* \frac{\tilde{A}}{C} \right|^2 + p_a \cdot p_f p_d \cdot p_e \left| \frac{A}{D} + \xi_2^* \frac{\tilde{A}}{D} \right|^2 - L(p_a, p_f, p_d, p_e) \Re X_2 + \varepsilon(p_a, p_f, p_d, p_e) \Im X_2 \right\} \quad (31)$$

(iii) $\underline{\bar{D}_i \bar{D}_j \rightarrow \bar{U}_k \bar{U}_l + \ell^+ \ell^+}$

$$\sum |\mathcal{M}|^2 = 128 \mathcal{K}^2 |V_{U_k D_i}^* V_{U_l D_j}^*|^2 p_a \cdot p_b \left\{ p_c \cdot p_e p_d \cdot p_f \left| \frac{A}{C} + \xi_3^* \frac{B}{F} \right|^2 + p_c \cdot p_f p_d \cdot p_e \left| \frac{A}{D} + \xi_3^* \frac{B}{E} \right|^2 - L(p_c, p_f, p_d, p_e) \Re X_3 + \varepsilon(p_c, p_f, p_d, p_e) \Im X_3 \right\} \quad (32)$$

where the following definitions have been used:

$$\begin{aligned} X_1 &= \left(\frac{A}{C} + \xi_1^* \frac{B}{E} \right) \left(\frac{A}{D} + \xi_1^* \frac{B}{F} \right)^* & \xi_1 &= V_{U_i D_l} V_{U_j D_k} / (V_{U_i D_k} V_{U_j D_l}) \\ X_2 &= \left(\frac{A}{C} + \xi_2^* \frac{\tilde{A}}{C} \right) \left(\frac{A}{D} + \xi_2^* \frac{\tilde{A}}{D} \right)^* & \xi_2 &= V_{U_i D_j} V_{U_l D_k} / (V_{U_i D_k} V_{U_l D_j}) \\ X_3 &= \left(\frac{A}{C} + \xi_3^* \frac{B}{F} \right) \left(\frac{A}{D} + \xi_3^* \frac{B}{E} \right)^* & \xi_3 &= V_{U_l D_i} V_{U_k D_j} / (V_{U_k D_i} V_{U_l D_j}) \end{aligned} \quad (33)$$

$$\begin{aligned} L(p_1, p_2, p_3, p_4) &= p_1 \cdot p_2 p_3 \cdot p_4 - p_1 \cdot p_3 p_2 \cdot p_4 + p_1 \cdot p_4 p_2 \cdot p_3, \\ \varepsilon(p_1, p_2, p_3, p_4) &= \varepsilon^{\mu\nu\lambda\rho} (p_1)_\mu (p_2)_\nu (p_3)_\lambda (p_4)_\rho \end{aligned} \quad (34)$$

with $\varepsilon^{0123} = +1$. The above formulas (30), (31), (32) have been written down in all generality allowing for possibility that the matrix elements of the CKM matrix might be complex. Except for s-channel contributions, such squared matrix elements were already given in [16] in the framework of the same model as that here used. However, the formulas found in [16] disagree from ours in various aspect, and in the fact that they seem to have been obtained as if a $(1 + \gamma^5)/2$ were used for the coupling between leptons, Majorana neutrinos and W^- , instead of the usual $(1 - \gamma^5)/2$ for left-handed coupling (formula (2) in [16] should then contain a $(1 + \gamma^5)/2$ factor). The numerical applications reported here concern only quarks of the first and second family and *for those* the elements of the CKM matrix can be approximated (Wolfenstein parameterization [31]) to a high degree of accuracy to be real. Accordingly ξ_1, ξ_2, ξ_3 will be real and $\Im X_1 = \Im X_3 = 0$. Only X_2 will retain an imaginary part due to the complex resonant propagator factors.

The decay width of the heavy neutrino, Γ_N , which appears in the factors \tilde{C} and \tilde{D} is of course a quantity which depends on the parameters of the particular model that is being considered here, B_{eN} and M_N . It receives contributions from the two decay channels $N_\ell \rightarrow W + \ell$ (charged current) $N_\ell \rightarrow Z + \nu_\ell$ (neutral current). In the present model there are no other decay channels open. Some authors however [17,18] include also possible Higgs interactions of the heavy neutrino states. Doing so will open up additional decay modes depending on the mass relation between M_N and M_H . As both of these parameters are still unknown the present authors prefer not to consider this possibility. Hence the values used for Γ_N in the present estimates of the resonant cross-sections should be regarded as *lower bounds* for the heavy neutrino total width. As the total decay width appears in the resonant propagator factors, it is a quite important parameter as regards numerical applications. Thus in appendix A are reported the formulas used to evaluate the partial and total decay widths, while in Table I the corresponding numerical values of the total decay width Γ_N are reported for different values of the neutrino mass M_N . It can be inferred that the total decay width changes quite drastically going from $\Gamma_N/M_N = 0.0011\%$ at $M_N = 100$ GeV to $\Gamma_N/M_N = 0.43\%$ at $M_N = 1000$ GeV. In addition it is to be remarked that the authors of [7] quote even smaller values of the total decay width (see Table I) which appear to be unsubstantiated within the present model. Using the interaction of Eq. (8) one readily evaluates in the unitary gauge the partial widths (assume $M_N \gtrsim 100$ GeV) $\Gamma(N_l \rightarrow W + l)$ and $\Gamma(N_l \rightarrow Z + \nu_l)$ and hence the total decay width. In the appendix it is shown explicitly that the values of the width quoted by the authors of ref. [7] can be reproduced by calculating in the 't Hooft gauge but not including the ghosts (Goldstone bosons) diagram.

In reference [5] in order to keep the numerical computations of cross-sections reasonably simple, a constant value of Γ_N was assumed. Here this is not possible as the width of the heavy neutrino varies so strongly between low (≈ 100 GeV) and high (≈ 1000 GeV) masses, and one is obliged to keep the functional dependence of the total width on the neutrino mass M_N . This makes the contribution of the resonant diagrams strongly dependent on the

heavy neutrino mass M_N .

IV. THE THIRD ORDER PROCESS $pp \rightarrow \ell^+ \ell^+ + W^-$

This process has been the object of [7] where the square of the amplitude and the subsequent phase-space integration were calculated by means of the COMPHEP package [8].

The amplitude of the third order process is:

$$\begin{aligned}
\mathcal{M} &= \mathcal{K}' \tilde{A}' \bar{v}(p_b) \gamma^\mu \frac{1 - \gamma_5}{2} u(p_a) \tilde{T}_{\mu\nu} [\epsilon'_{(\lambda)}(Q)]^* \\
\mathcal{K}' &= \left(\frac{g}{\sqrt{2}} \right)^3 V_{ud}^* B_{eN}^2 M_N \\
1/\tilde{A}' &= [(p_a + p_b)^2 - M_W^2 + iM_W \Gamma_W] \\
\tilde{C}' &= (p_e + Q)^2 - M_N^2 + iM_N \Gamma_N, \\
\tilde{D}' &= (p_f + Q)^2 - M_N^2 + iM_N \Gamma_N,
\end{aligned} \tag{35}$$

with $\tilde{T}_{\mu\nu}$ defined in Eq. (20). Clearly relative to the annihilation amplitude of the process $u \bar{d} \rightarrow \ell^+ \ell^+ + u \bar{d}$, given in Eq. (18), the outgoing quark's current $[\tilde{J}'_{(c,d)}]^*$ is replaced by the on-shell W gauge boson polarization vector $[\epsilon'_{(\lambda)}(Q)]^*$ and the constants \tilde{A}' and \mathcal{K}' are accordingly redefined.

Here a formula is given which was derived by means of the standard method of squaring the amplitude and summing over polarizations of initial and final particles thus reducing the calculation to the product of traces of strings of Dirac matrices.

$$\begin{aligned}
\sum_{\text{spins}} |\mathcal{M}|^2 &= 16 |\mathcal{K}' \tilde{A}'|^2 \\
&\times \left\{ \frac{1}{|\tilde{C}'|^2} p_a \cdot p_e \left(p_b \cdot p_f + 2 \frac{Q \cdot p_f Q \cdot p_b}{M_W^2} \right) + \frac{1}{|\tilde{D}'|^2} p_a \cdot p_f \left(p_b \cdot p_e + 2 \frac{Q \cdot p_e Q \cdot p_b}{M_W^2} \right) \right. \\
&+ \Re e \left(\frac{1}{\tilde{C}' \tilde{D}'^*} \right) \left[p_e \cdot p_f \left(p_a \cdot p_b + 2 \frac{Q \cdot p_a Q \cdot p_b}{M_W^2} \right) - p_a \cdot p_f \left(p_b \cdot p_e + 2 \frac{Q \cdot p_e Q \cdot p_b}{M_W^2} \right) \right. \\
&\left. \left. - p_a \cdot p_e \left(p_b \cdot p_f + 2 \frac{Q \cdot p_f Q \cdot p_b}{M_W^2} \right) \right] - \Im m \left[\frac{\varepsilon(p_a, p_f, p_b, p_e)}{\tilde{C}' \tilde{D}'^*} \right] \left(1 + 2 \frac{Q \cdot p_b}{M_W^2} \right) \right\}, \tag{36}
\end{aligned}$$

where Q is the W boson four-momentum. It should also be remarked that the above result has been verified against that of the annihilation part of Eq. (28) by taking the small width

approximation on the latter, factorizing the phase-space and integrating out that of the two quarks from the on-shell W .

However the formula given by the authors of ref. [7] (c.f in the appendix) appears not to take into account the fact that the amplitude is the sum of two diagrams antisymmetrized with respect to the variables of the two identical leptons in the final state. The two diagrams have different heavy Majorana neutrino propagator factors (c.f \tilde{C}' and \tilde{D}' in Eq. (35)). Moreover all factors explicitly dependent on $(M_W^2)^{-1}$ and coming from the sum over the real W polarizations $[\sum_\lambda \epsilon_\lambda(k)\epsilon_\lambda^*(k) = -\eta_{\mu\nu} + (k_\mu k_\nu)/M_W^2]$ are missing. They claim that their result is the output of the COMPHEP software package [8] which allowed them to perform symbolic computation of matrix elements. In order to understand the reason of this discrepancy the present authors decided to verify again the result given in Eq. 36 by using the same COMPHEP software package used by the authors of ref. [7]. It appears that in COMPHEP non standard models have to be defined, in the sense that new particles and new interaction vertices have to be defined by the user. COMPHEP can perform calculations both in the unitary gauge and in the 't Hooft gauge. Defining the heavy neutrino and its interactions as in Eq. (8) and working in the *Unitary gauge* it has been verified that the COMPHEP output reproduces that reported in Eq. (36) up to the factor containing the totally antisymmetric Levi-Civita tensor: this is because the program directly replaces the squared propagator for the resonant particles. However, adding this term to the COMPHEP fortran output of the matrix elements, it is found numerically irrelevant as it is proportional to the width of the heavy neutrino N . It is thus established that Eq. (36) agrees with the COMPHEP output in the unitary gauge up to terms proportional to the width of the resonant particle (neutrino).

Working with COMPHEP in the *'t Hooft gauge* requires some care as in this gauge also the couplings of the W^\pm and Z Goldstone bosons (ghosts) have to be defined by the user. These are necessary to reproduce the correct sum over polarizations for W^\pm and Z . With the inclusion of the ghost vertices the calculation in the 't Hooft gauge reproduces the result of the Unitary gauge (as it should) which agrees with that of Eq. (36). Doing so the

present authors realized that the result of ref. [7] [c.f. Eq. (A1)] is indeed obtained with the COMPHEP package working in the 't Hooft gauge if one *does not defines the ghost vertices*. The discrepancy of the result of this report, Eq. (36), with that of Eq.(A1) of ref. [7] is thus resolved: the formula given in ref. [7] is just one of the terms when working in the 't Hooft gauge; the ghost contribution needs to be added to get the complete result which agrees with that reported here in Eq. (36) which is obtained in the unitary gauge.

In the appendix formulas are presented which illustrate this point explicitly for the simpler case of the heavy neutrino width. The calculation without including the ghost diagrams amounts to use $[\sum_{\lambda} \epsilon_{\lambda}(k)\epsilon_{\lambda}^*(k) = -\eta_{\mu\nu}]$ for the sum over the gauge boson polarizations and the width thus obtained reproduces the anomalously small values reported in ref. [7] for $M_N = 100, (800) \text{ GeV}$.

The total cross-section, summing up the contributions of the quarks of the first and second generations, is given by:

$$\sigma = \frac{1}{2\hat{s}} \int dx_a dx_b \sum_{U\bar{D}} [f_U(x_a)f_{\bar{D}}(x_b) + x_a \leftrightarrow x_b] \times \frac{1}{4} \times \frac{1}{3} \sum_{\text{spins}} |\mathcal{M}|^2(U\bar{D} \rightarrow e^+e^+W) \frac{d_3\text{LIPS}(\sqrt{\hat{s}}; p_e, p_f, Q)}{2}, \quad (37)$$

where the numerical factors account for average on initial spins and colors. All numerical results presented in the next section will be at the level of a parton Monte Carlo, while aspects like jet hadronization and detector simulations are beyond the scope of this work.

V. DISCUSSION AND RESULTS

The previous observation clearly does not affect the W-W fusion matrix elements because in the t-channel there is no finite width effect and the gauge boson propagator's numerator is simply $\eta_{\mu\nu}$ also in unitary gauge as the limit of massless external particles is assumed. As stated, correctly, in ref. [7] these diagrams give rise to a very small cross-section, $\sigma \simeq 10^{-5} - 10^{-4} \text{ fb}$ in the range of neutrino masses of interest here $100 \text{ GeV} \leq M_N \leq 1000 \text{ GeV}$. At the LHC assuming an integrated luminosity over one year of $L = 100 \text{ fb}^{-1}$ one could define

a minimal cross-section $\sigma_0 = 10^{-2}$ fb that would give 1 event per year. Clearly, smaller cross-section would be impossible to measure (with statistical significance) on a one year run. Thus, for the model studied in this work, the WW-fusion mechanism is negligible and not measurable. This was checked : (i) with authors' defined fortran code [6] based on Eqs. (30,31,32) and feeding them into the phase space integration routines provided within the COMPHEP package; (ii) and directly with COMPHEP performing a symbolic matrix element calculation followed by numerical (VEGAS) phase space integration.

Therefore the following discussion will concentrate on the resonant production mechanism of Fig. 2, with a particular emphasis on the third order process and the comparison with the result reported in [7]. The following numerical results were obtained with COMPHEP, using the same kinematic cuts of ref. [7]: $p_T^{lepton} > 5$ GeV, $p_T^W > 15$ GeV and $|\eta| < 2.5$ for the final state particles. The parton distributions functions (PDF) used are the set of MRS[G] [32]. As shown explicitly in [6] these type of calculations are not very sensitive to the particular choice of PDF as long as one restrict itself to the more recent sets.

Notwithstanding the differences highlighted in the previous section regarding the analytic formula of the matrix element and of the total width, the numerical value of the total cross-section is within $\approx 20\%$ of that reported in [7] as can be seen in Fig. 3: this can be easily understood as the cross-section could be written, to a good approximation, as a product of the production cross-section $\sigma(pp \rightarrow \ell^+ N)$ (independent from Γ_N), times the branching ratio $\Gamma(N \rightarrow \ell^+ W^-)/\Gamma_N$ that is numerically the same although the formulas are different.

Differences are however found on angular distributions of decay products (leptons and/or jets), that may be very important for the detection of the signal. Notice that from theoretical arguments [33] it can be stated that a forward-backward symmetry should show up in processes of production of heavy Majorana through CP conserving interactions like that here considered. Figs. 4&5 show normalized angular distributions of the outgoing lepton(s) and gauge boson. Let Θ_ℓ (Θ_W) be the angle formed by \vec{p}_ℓ (\vec{p}_W) with the positive direction of the collision axis, in the center of mass system (c.m.s.) of the hadronic (pp) reaction (lab frame). Figs. 4&5 show the expected forward-backward symmetric behavior and in

particular that the final state particles are emitted preferentially parallel or anti-parallel to the collision axis. Fig. 6 shows the normalized distribution in the opening angle of the two like sign leptons. Here a difference is found relative to the numerical results reported in ref. [7]. In Fig. 6 one can observe that for relatively low neutrino masses the two leptons are emitted preferentially parallel to each other while at high neutrino masses the distribution tends to become flatter.

The opposite behaviour is instead predicted in ref. [7] (see their Fig. 5). This can again be explained assuming the interpretation given above of the calculation reported in [7]. The absence of the ghost particles amounts to the absence of the longitudinal polarization of the W-gauge boson ($J_z^W = 0$): so the W gauge boson would have only the two helicity states $\lambda = \pm 1$. Suppose a head-on collision between a u and \bar{d} with \vec{p}_u along the positive direction of the z axis. As u has $\lambda = -\frac{1}{2}$ and \bar{d} has $\lambda = +\frac{1}{2}$, the initial total angular momentum is $J_z = -1$. To conserve angular momentum along the z axis, the only allowed configuration in the final state, composed of the two identical leptons and an on-shell W , is with a W-gauge boson with $\lambda = -1$ and the two positrons emitted with opposite momentum (antiparallel), since the two leptons have the same helicity, to give $J_z^{\ell\ell} = 0$. If we start with $\bar{d} u$ we have an initial $J_z = +1$, so the final W has $\lambda = +1$ and the two leptons are again emitted antiparallel. However in reality the W-gauge boson has also the longitudinal polarization and the $J_z^W = 0$ possibility is also present: when this is so, the two leptons must be parallel to give $J_z^{\ell\ell} = \pm 1$. This additional helicity amplitude prevents the angular distribution to drop as $\theta_{\ell\ell} \rightarrow 0$.

The other distributions discussed in ref. [7] (c.f. transverse W-mass, transverse W-momentum and invariant mass $M_{\ell W}, M_{\ell\ell W}$) are confirmed by the present calculations and so are not repeated in this report. Fig. 7 shows the angular distribution with respect to the opening angle of the jets in the fourth order process. It is worth noticing that the W-angular-distribution, Fig. 5, is more strongly peaked along the collision axis than that of the leptons, Fig. 4. Thus the jets that originate from its decay are expected to be emitted preferentially along the collision axis and parallel to each other. This is indeed confirmed by the parton

level simulation as shown in Fig. 7. If one takes into account that in the hadronization process more than two jets may be present, it is clear that the mass reconstruction of the W may not be so easy from the experimental point of view.

The peculiar characteristics of the signal are: two like sign leptons with the same angular and transverse momentum distributions, no missing energy, and at least two jets with an invariant mass distribution peaked at the W mass while the invariant mass distributions in the $jj\ell$ system will be peaked at the heavy neutrino mass, as shown in [7]. Clearly no SM process have these features but some have final states with accompanying neutrinos (missing energy) which are a source of potential background to the LSD + 2jets signal. All previously cited literature considered only heavy quark ($t\bar{t}$, $b\bar{b}$) production and subsequent decay as a major source. However recent simulations [34] have recognized that more dangerous background at LHC can be single top production and gauge boson pair production (WZ and ZZ) followed by leptonic decays. After all cuts (for details see ref. [34]) the authors find a background of 4.9 ± 1.6 events with an integrated luminosity of 10 fb^{-1} that implies a total cross $\sigma \simeq 0.5 \text{ fb}$. This would restrict the observability of the signal studied here in the neutrino mass range $100 - 250 \text{ GeV}$. However the kinematic cuts used here are softer than those used for the SM background suppression in ref. [34], so it is interesting to understand if the conclusions above can be significantly affected by changing the kinematic cuts. In [34] is indicated that at least a cut of 40 GeV on p_T^{lepton} is necessary to suppress the SM background (also an isolation cut is needed but this will not affect the signal significantly). In Fig. 3 the dashed curve shows the effect on the signal of increasing the cut on the p_T^{lepton} up to 40 GeV : the total cross-section is lowered by a factor of up to an order of magnitude in the region of low neutrino masses, but it is practically unchanged in the high mass region. The drastic change in shape found at small masses can be qualitatively understood by noticing that when M_N is small a larger part of the energy goes into M_W mass leaving not much kinetic energy for the outgoing particles, so a high cut on p_T naturally lowers the cross-section. This is in agreement with the lepton transverse momentum distributions (which are not reported here as they are the same of those reported in ref. [7]): these are peaked

at $p_T^{lepton} \approx M_N/2$. Clearly a cut of 40 GeV on p_T^{lepton} cuts away most of the events when $M_N \approx 100$ GeV, thus causing a drastic change in σ_{tot} . However it should be remarked that also within these strong cuts there still remain a measurable number of events.

VI. CONCLUSIONS

This paper has addressed the lepton number violating processes (i) $pp \rightarrow \ell^+ \ell^+ + 2\text{jets}$ and (ii) $pp \rightarrow \ell^+ \ell^+ W^-$ within the scenario of models where heavy Majorana neutrinos mix with light leptons. In particular regarding the fourth order process (i) explicit analytic expressions of the helicity amplitudes are provided for the two competing mechanisms: the WW-fusion and the resonant neutrino production. These helicity amplitudes might also be useful for more realistic (detector dedicated) Monte Carlo simulations and/or within the scenario of other models beyond the standard electroweak theory. With respect to process (ii) a detailed study, both analytical and numerical, with a thorough comparison to the work of ref. [7], has been performed finding some differences in the analytical formula of the matrix element which have been explained by noticing that the formula given in ref. [7] does not include the ghost contribution needed in the Feynman-'t Hooft gauge. However, as important as this might be, the main conclusion of ref. [7] (the size of σ_{tot}) is only affected by an error of $\approx 20\%$, though relevant differences are found on some of the angular distributions.

In particular the distribution in the opening angle ($\Theta_{\ell\ell}$) of the two leptons (Fig. 6) is found to be significantly different from that reported in [7].

According to the study presented here in the framework of the mixing model of heavy left-handed neutrinos there is a mass range of up to $M_N \approx 800$ GeV where the cross-section would be in principle observable (1 event per year assuming an integrated luminosity of 100 fb^{-1}). This window in the heavy neutrino masses is drastically reduced down to $M_N \approx 250$ GeV taking into account the recent SM background estimates quoted in ref. [34] ($\approx 50 \pm 16$ events/year with an integrated luminosity of 100 fb^{-1}), which appears to be dominated by the production of double gauge bosons and single top.

The observation of the LSD signal, in this model, is thus ultimately related to the size of the mixing angle and the possibility of suppressing the SM background. If a like sign dilepton signal will be seen at LHC, then the question of determining the underlying physics scenario, that triggers the non SM signal, would immediately arise; more realistic, detector dedicated, Monte Carlo simulations would be needed and, of course, this eventuality would require additional theoretical work. It is the authors' belief that the present work would in any case be of importance in this direction.

ACKNOWLEDGMENTS

C. C. acknowledges support of an INFN grant (PG-102061/2000) that allowed his stay in Perugia.

APPENDIX: TOTAL DECAY WIDTH OF THE HEAVY NEUTRINO

The expression for the partial decay widths of the heavy neutrino states as deduced from the interaction Lagrangian given in Eq. (8) are given by:

$$\Gamma(N_\ell \rightarrow W\ell) = \frac{\alpha}{16 s_W} \frac{M_N^3}{M_W^2} |B_{eN}|^2 \Phi(x_W), \quad (\text{A1})$$

$$\Gamma(N_\ell \rightarrow Z\nu_\ell) = \frac{\alpha}{16 s_W} \frac{M_N^3}{M_W^2} |B_{eN}|^2 |B_{\nu N}|^2 \Phi(x_Z), \quad (\text{A2})$$

with $\Phi(x) = (1-x)^2(1+2x)$, $x_{W,Z} = M_{W,Z}^2/M_N^2$ and $s_W = \sin^2 \theta_W$, where θ_W is the Weinberg angle, α the fine structure constant and $|B_{\nu N}|^2$ is determined from Eqs. (9).

The total decay width is given by

$$\Gamma_N = 2 \Gamma(N_\ell \rightarrow W\ell) + \Gamma(N_\ell \rightarrow Z\nu_\ell) \quad (\text{A3})$$

The factor of two in Eq. (A3) arises because, due to its Majorana nature, the heavy neutrino can decay into $W^{-\ell^+}$ and $W^{+\ell^-}$ *with equal probability*. In Table I, the corresponding numerical values are reported for the total decay width Γ_N . Including Higgs interactions of the heavy Majorana states will increase the neutrino total decay width Γ_N .

The formulas that reproduce the widths given in [7], as explained in the text, are obtained using 't Hooft-Feynman gauge but *without* including the Goldstone boson contribution, which amounts to use for the sum over the real W polarizations: $\sum_{\lambda} \epsilon_{\lambda}(k) \epsilon_{\lambda}^*(k) = -\eta_{\mu\nu}$, i.e. that corresponding to a massless gauge boson. One finds:

$$\Gamma(N_{\ell} \rightarrow W\ell) = \frac{\alpha}{8 s_W} M_N |B_{eN}|^2 \Pi(x_W), \quad (\text{A4})$$

$$\Gamma(N_{\ell} \rightarrow Z\nu_{\ell}) = \frac{\alpha}{8 s_W c_W} M_N |B_{eN}|^2 |B_{\nu N}|^2 \Pi(x_Z), \quad (\text{A5})$$

with $\Pi(x) = (1 - x)^2$ and $c_W = \cos^2 \theta_W$, which indeed reproduce the values of Γ_N given by [7] and reported in table I.

REFERENCES

- [1] B. Baller [DONUT Collaboration], Nucl. Phys. Proc. Suppl. **98**, 43 (2001).
K. Kodama *et al.* [DONUT Collaboration], Phys. Lett. B **504**, 218 (2001).
- [2] Y. Fukuda et al. (Super-Kamiokande), Phys. Rev. Lett. **81**, 1562-1567, 1998
- [3] O. Panella and Y. N. Srivastava, Phys. Rev. D **52**, 5308-5313, 1995.
- [4] O. Panella (1995), hep-ph/9509390
- [5] O. Panella, C. Carimalo, Y. N. Srivastava and A. Widom, Phys. Rev. D **56**, 5766-5775, 1997.
- [6] O. Panella, C. Carimalo, Y. N. Srivastava, Phys. Rev. D **62**, 015013, 2000.
- [7] F. M. L. Almeida Jr, Y. A. Coutinho, J. A. Martins Simões and M. A. B. do Vale, Phys. Rev. D **62** 075004 (2000).
- [8] A. Pukov, E. Boos, M. Dubinin, V. Edneral, V. Ilyn, D. Kovalenko, A. Kryukov, V. Savrin, S. Shichanin, A. Semenov. User's manual for version 33: hep-ph/9908288
- [9] W. Buchmüller, C. Greub, Nucl. Phys. **B 363**, 345 (1991).
- [10] C. A. Heusch, P. Minkowski, Nucl. Phys. **B 416**, 3 (1994).
- [11] M. Gell-Mann, P. Ramond, R. Slansky, in *Supergravity*, eds. P. van Nieuwenhuizen e D. Friedman, North-Holland, Amsterdam (1979);
T. Yanagida, *Proc. Workshop on unified theory and baryon number of the Universe*, eds. O. Sawada and A. Sugamoto, KEK, Japan (1979).
- [12] R. N. Mohapatra, G. Senjanović, Phys. Rev. **D 23**, 165 (1981).
- [13] A. Pilaftsis, Z. Phys. **C 55**, 275 (1992); e-Print archive: hep-ph/991206.
- [14] W. Buchmüller, D. Wyler, Phys. Lett. **B 249**, 458 (1990).
- [15] L. N. Chang, D. Ng, J. N. Ng, Phys. Rev. **D 50**, 4589 (1994).

- [16] D. A. Dicus, D. D. Karatas, P. Roy Phys. Rev. D **44**, 2033 (1991).
- [17] A. Datta, M. Guchait, A. Pilaftsis, Phys. Rev. D **50**, 3195 (1994).
- [18] J. Gluza, M. Zrałek, Phys. Rev. D **55**, 7030 (1997).
- [19] R. N. Mohapatra, J. W. F. Valle, Phys. Rev. D **34**, 1642 (1986).
- [20] J. Bernabéu et al., Phys. Lett. **B 187**, 303 (1987).
- [21] D. Tommasini, G. Barenboim, J. Bernabéu, C. Jarlskog, Nucl. Phys. **B 444**, 451 (1995).
- [22] I. Melo, e-Print archive: hep-ph/9612488;
P. Kalyniak, I. Melo, Phys. Rev. D **55**, 1453 (1997).
- [23] M. C. Gonzalez-Garcia, J. W. F. Valle, Phys. Lett. **B 216**, 360 (1989).
- [24] J. Schechter, J. W. F. Valle, Phys. Rev. D **22**, 2227 (1980).
- [25] Y. F. Pirogov, hep-ph/0005290.
- [26] A. Ilakovac, A. Pilaftsis, Nucl. Phys. **B 437**, 491 (1995).
- [27] E. Nardi, E. Roulet, D. Tommasini, Phys. Lett. **B 327**, 319 (1994);
E. Nardi, E. Roulet, D. Tommasini, Phys. Lett. **B 344**, 225 (1995).
- [28] G. Bélanger, F. Boudjema, D. London and H. Nadeau, Phys. Rev. D **53**, 6292 (1996).
- [29] K. Choi and A. Santamaria, Phys. Lett. **B 267**, 504 (1991).
- [30] R. Kleiss and W. J. Stirling, Nucl. Phys. **B 262** (1985) 235-262.
- [31] L. Wolfenstein, Phys. Rev. Lett. **51**, 1945 (1983).
- [32] A. D. Martin, R. G. Roberts and W. J. Stirling, Phys. Lett. **B 354**, 155 (1995).
- [33] S. T. Petcov, Phys. Lett. **B 319**, 421 (1984).
- [34] H. Dreiner, P. Richardson and M. Seymour, Phys. Rev. D **63**, 055008 (2001).

TABLES

TABLE I. Total decay width of the (electron) heavy neutrino $\Gamma_N = \Gamma(N \rightarrow W\ell) + \Gamma(N \rightarrow Z\nu)$, obtained through the use of Eq. (A1) and Eq. (A2) with $B_{eN} = 0.0052$.

$M_N(\text{GeV})$	100	300	500	600	800	1000
$\Gamma_N(\text{GeV})$	0.11×10^{-2}	$0.138 \times 10^{+0}$	$0.65 \times 10^{+0}$	$1.13 \times 10^{+0}$	$0.267 \times 10^{+1}$	$0.52 \times 10^{+1}$
$\Gamma_N(\text{GeV})^a$	0.650×10^{-3}	-	-	-	0.580×10^{-1}	-

^aFor comparison the values used by the authors of [7] are also reported.

FIGURES

FIG. 1. W fusion mechanism for production of Like-Sign-Dileptons (LSD) in high energy hadronic collisions. These diagrams, including the appropriate exchanges, describe also quark quark scattering and anti-quark anti-quark scattering.

FIG. 2. Production of LSD through quark anti-quark scattering. In addition to the diagram of Fig. 1 (virtual W fusion), one must consider the $\ell^+ N_\ell$ production via quark anti-quark annihilation with subsequent hadronic decay of the heavy neutrino $N_\ell \rightarrow \ell^+ q \bar{q}$ ($\ell = e, \mu, \tau$). In principle for $q \bar{q}$ this process interferes with the one in Fig. 1.

FIG. 3. Signal cross-section for $pp \rightarrow \ell^+ \ell^+ W^-$ ($\ell = e$): the solid line includes contributions from first and second generation quarks; the dot-dashed line includes only the $u \bar{d}$ contribution which is clearly the dominant (90%); the dashed line indicates the total cross-section when a higher cut on the lepton transverse momentum $p_T > 40$ GeV is applied.

FIG. 4. Lepton polar angle (Θ_ℓ) distribution in the third order process $pp \rightarrow e^+ e^+ W^-$ at LHC energy $\sqrt{S} = 14$ TeV, for different values of the heavy neutrino mass M_N . Θ_ℓ is the *laboratory polar angle* i.e. the angle formed by the lepton with the positive direction of the hadronic collision axis.

FIG. 5. Distribution in the gauge boson W^- polar angle (Θ_W) in the third order process $pp \rightarrow e^+ e^+ W^-$ at LHC energy $\sqrt{S} = 14$ TeV, for different values of the heavy neutrino mass M_N . The same legend as in Fig 4 applies. The polar angle Θ_W is defined in the laboratory system i.e. with respect to the hadronic collision axis.

FIG. 6. Distribution in the opening angle between the two identical leptons ($\Theta_{\ell\ell}$), defined in the laboratory frame, in the third order process $pp \rightarrow e^+e^+W^-$ at LHC energy $\sqrt{S} = 14$ TeV. The legend of Figure 4 applies.

FIG. 7. Fourth order process $pp \rightarrow e^+e^+2jets$. Distributions for the opening angle (in the laboratory frame) between the two quarks (jets) (Θ_{jj}) coming from the W^- gauge boson decay. The different curves refer to different values of the heavy neutrino mass according to the legend of Figure 4.

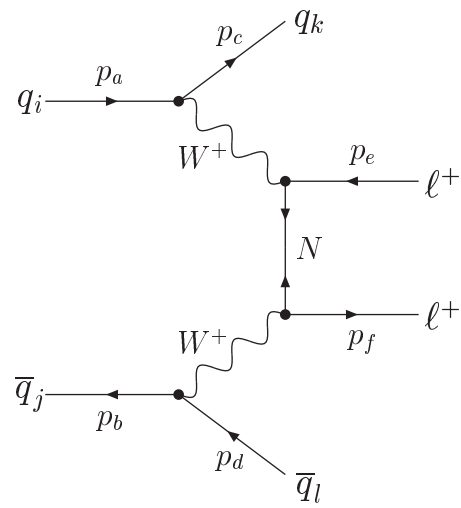


Fig. 1

PANELLA *et al.*

Physical Review D

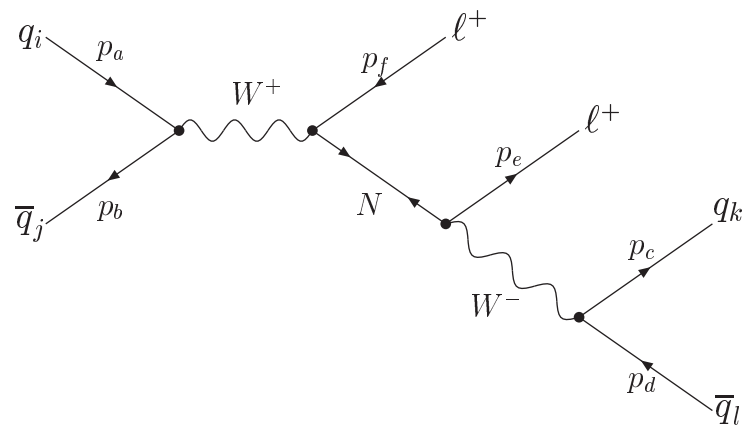


Fig. 2

PANELLA *et al.*

Physical Review D

Fig. 3
Panella et al.
Physical Review D

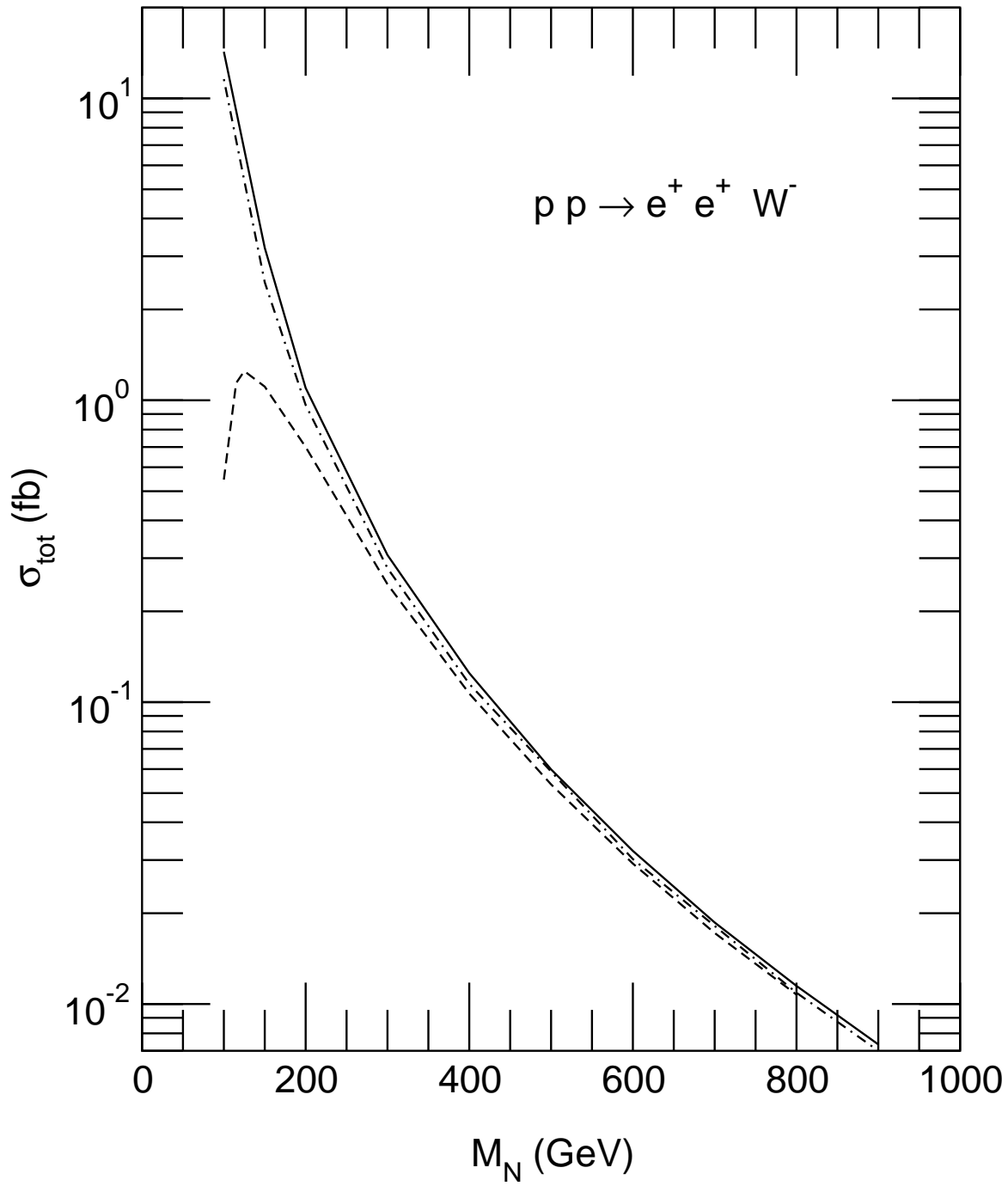


Fig. 4
Panella et al.
Physical Review D

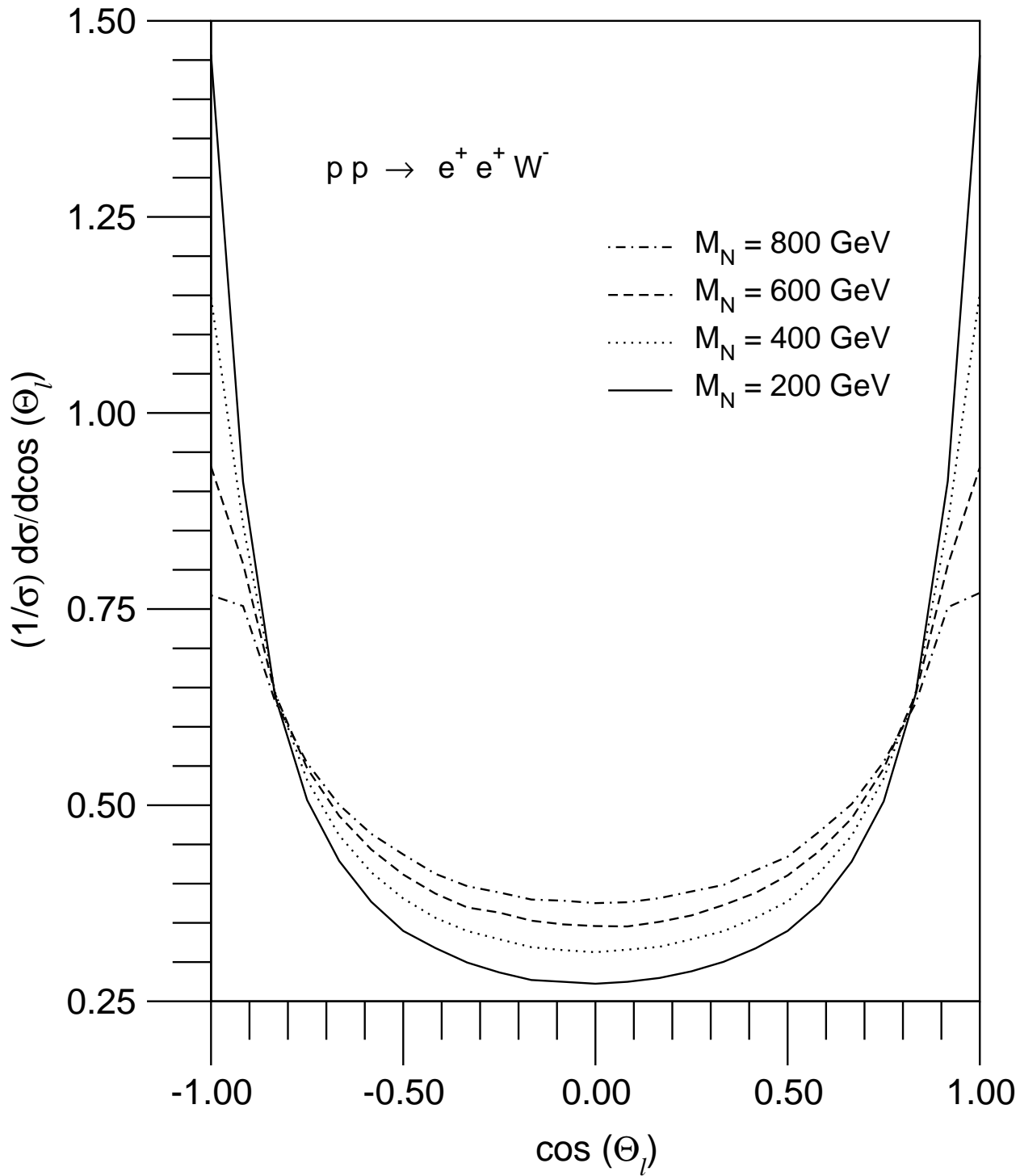


Fig. 5
Panella et al.
Physical Review D

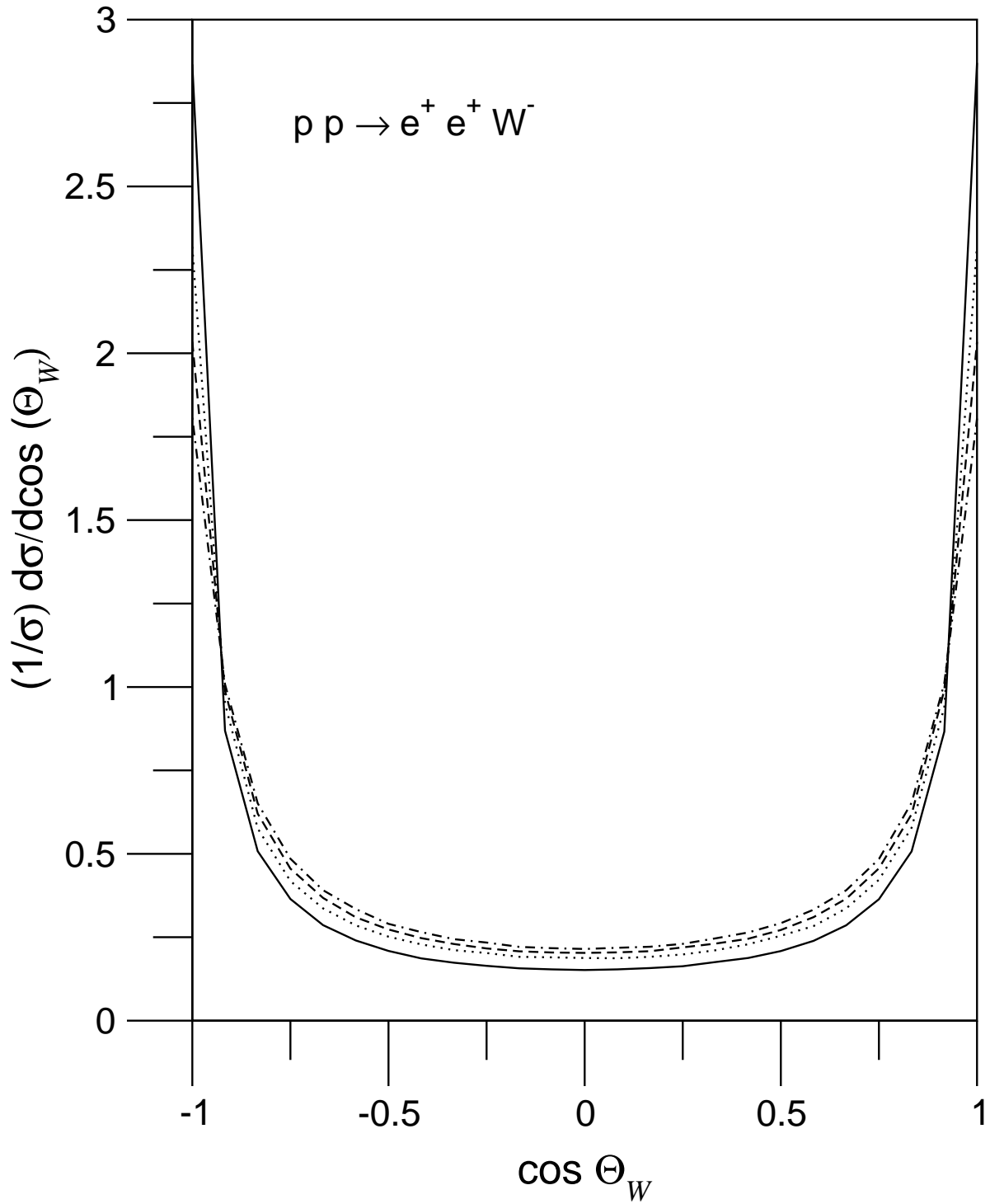


Fig. 6
Panella et al.
Physical Review D

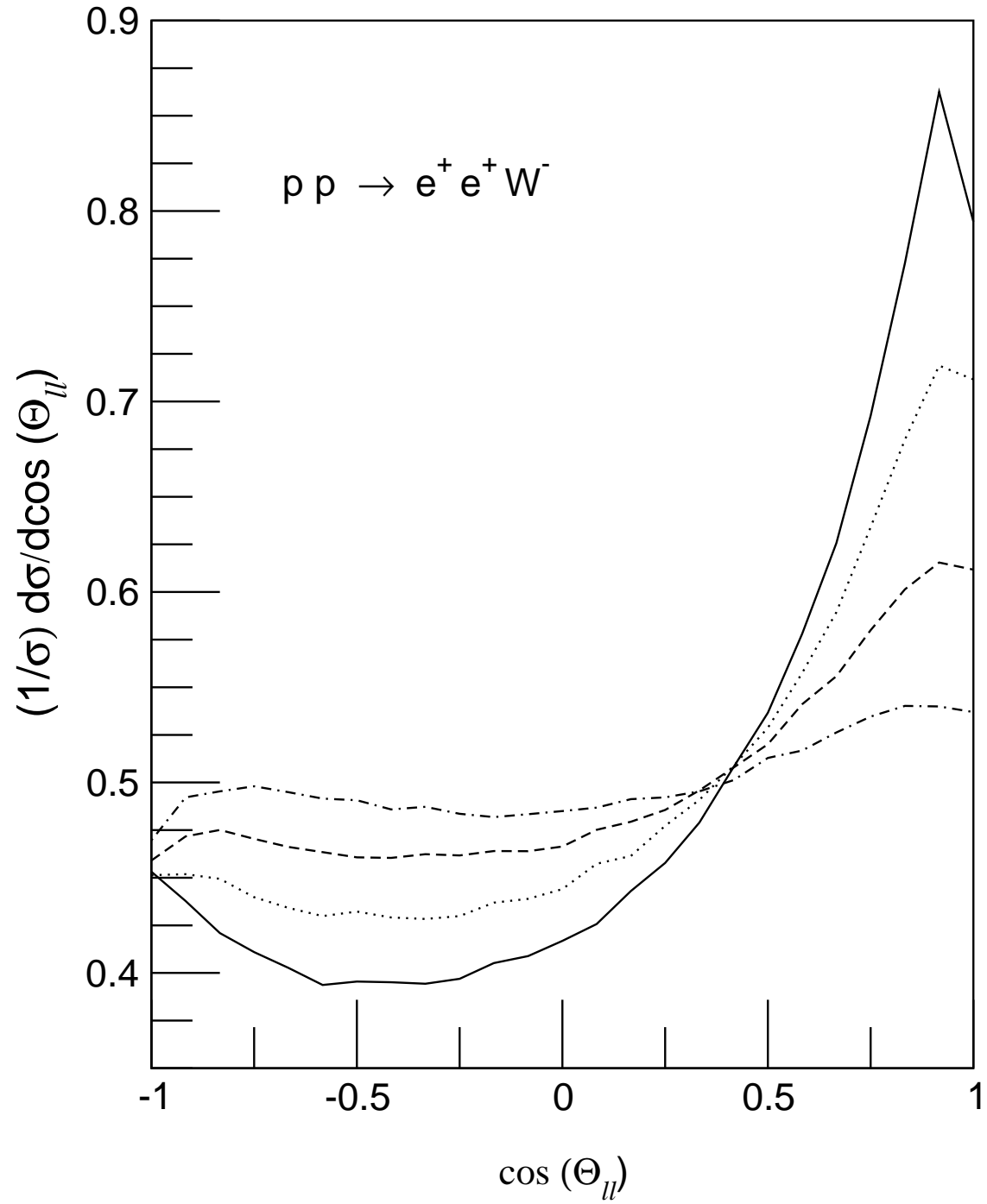


Fig. 7
Panella et al.
Physical Review D

